Temperature dependence of the Cr^{3+} site axial distortion in $LiSrAlF_6$ and $LiSrGaF_6$ single crystals

2001 J. Phys.: Condens. Matter 13 8435

(http://iopscience.iop.org/0953-8984/13/36/315)

INSTITUTE OF PHYSICS PUBLISHING JOURNAL OF PHYSICS: CONDENSED MATTER

J. Phys.: Condens. Matter **13** (2001) 8435–8443 PII: S0953-8984(01)26127-X

Temperature dependence of the Cr^{3+} site axial distortion in $LiSrAlF_6$ and $LiSrGaF_6$ single crystals

A N Medina[1], A C Bento[1], M L Baesso[1], F G Gandra[2], T Catunda[3] and A Cassanho[4]

[1] Departamento de Física, Universidade Estadual de Maringá, Avenida Colombo 5790, Maringá-PR, 87020-900, Brazil
[2] Instituto de Física Gleb Wataghin, Universidade Estadual de Campinas, 13083-970 Campinas-SP, Brazil
[3] Instituto de Física de São Carlos, Universidade de São Paulo, Avenida Dr Carlos Botelho 1465, São Carlos, SP 13560-250, Brazil
[4] AC Materials, 2721 Forsyth Road, Winter Park, FL 32792, USA

Received 25 June 2001
Published 23 August 2001
Online at stacks.iop.org/JPhysCM/13/8435

Abstract

The electron spin resonance (ESR) of Cr^{3+} in $LiSrAlF_6$ (LiSAF:Cr) and $LiSrGaF_6$ (LiSGaF:Cr) single crystals has been measured in the temperature range between 270 and 470 K. The external magnetic field orientation dependence of the spectra is described by a spin Hamiltonian of axial symmetry for both compounds. The value of the zero-field splitting axial parameter (D) for LiSGaF:Cr decreases from 6.60×10^{-2} cm^{-1} to 5.60×10^{-2} cm^{-1}, while for LiSAF:Cr it increases from 1.30×10^{-2} cm^{-1} to 1.60×10^{-2} cm^{-1} for increasing temperature. The larger values of D obtained for LiSGaF:Cr show that the distortion of the octahedral Cr site is greater in this compound, in agreement with x-ray diffraction results reported in the literature.

1. Introduction

Single crystals of the colquiriite fluoride family, $LiAMF_6$ (A = Ca, Sr and M = Al, Ga), have been reported as efficient broadly tunable laser materials when doped with Cr^{3+} [1–6]. Among all these materials, the compound $LiCaAlF_6$:Cr (LiCAF:Cr) is most robust and features more advantageous thermo-optical properties. It presents the highest melting temperature, thermal conductivity, emission lifetime and quantum efficiency. However, crystals of this material also present higher scattering and smaller absorption and emission cross section as compared to compounds with Sr. Consequently, the present consensus is that materials prepared with Sr are more promising candidates for laser systems. A comparison between the Al and Ga materials shows that for the infrared region they have nearly the same absorption band intensity and a similar emission cross section (4.8×10^{-20} cm^2 for LiSAF:Cr and 3.3×10^{-20} cm^2 for LiSGaF:Cr). They also have comparable fluorescence lifetime (67 and 88 μs for LiSAF:Cr

and LiSGaF:Cr, respectively) and the same slope efficiencies (∼50%) [7]. Despite these similarities, small differences were observed in the thermal properties of these two crystals: LiSGaF:Cr has a smaller thermal expansion coefficient, with a smaller anisotropy and a larger thermal conductivity, which makes it potentially more attractive for high-power laser applications [8, 9]. Recently, it has been shown that the thermal quenching of fluorescence is a very important mechanism to explain the different performance and the temperature behaviour of the lasers built with these materials [10].

In this family of compounds, all the metal cations occupy a distorted octahedral site between hexagonally close-packed layers of F atoms [11–14]. For the M site, occupied by Cr^{3+} in doped materials, the distortion is associated with the relative rotations of the two opposite trigonal F faces. As a result the symmetry is lowered from O_h to D_3. This static distortion has a significant effect on the physical proprieties of this system and fully accounts for the polarized nature of the absorption and emission spectra. The dynamical distortions also provide a contribution to the absorption strength and the emission lifetime [2, 15]. That is why it is important to investigate LiSGaF:Cr and LiSAF:Cr single crystals by the electron spin resonance (ESR) technique, which can be very sensitive to low-symmetry distortions.

Recently, ESR [16] was used to study low-symmetry distortions of the Cr site in $LiSr_xCa_{1-x}AlF_6$, where the ESR spectra clearly show that the zero-field splitting decreases with increasing Sr content at low temperatures. Although the optical spectrum is not very sensitive to the distortions of the octahedron [17], there are important consequences for the physical properties of these materials when used as laser-active media.

In this work, we report the ESR results of Cr^{3+} in $LiSrAlF_6$ and $LiSrGaF_6$ single crystals at high temperature (between 270 and 470 K), which is the working temperature range of the lasers built with these crystals. The small linewidth of the Cr^{3+} ESR spectrum enables one to study the temperature dependence of the spin Hamiltonian parameters, particularly the zero-field splitting parameter (D). The possible reasons for the distinct temperature dependence of D parameters are discussed.

2. Experimental aspects

2.1. Experimental procedure

The $LiSrAlF_6$ and $LiSrGaF_6$ single crystals, doped with 1.5 at.% of Cr^{3+}, were grown by the Czochralski technique reported in [18]. Their structure and orientation were verified using x-ray diffraction and absorption spectra. The ESR experiments were carried out at 9.5 GHz (X-band) with 0.5 mW power, using 100 kHz magnetic field modulation in the temperature range between 270 and 470 K.

2.2. Experimental results

The ESR spectra of LiSGaF:Cr at room temperature are shown in figure 1 for different angles relative to the c-axis. There are three well-resolved groups of lines observed for the magnetic field along the c-direction. Each group is composed of a central line and four satellite lines. The three central lines are due to the fine structure ($S = 3/2$) and the four satellites are due to the hyperfine structure ($I = 3/2$). No superhyperfine structure due to the interaction with F ions was observed. The angular dependence of the three principal lines ($I = 0$) is shown in figure 2(a), and no angular dependence was observed for the *ab*-plane, not shown here.

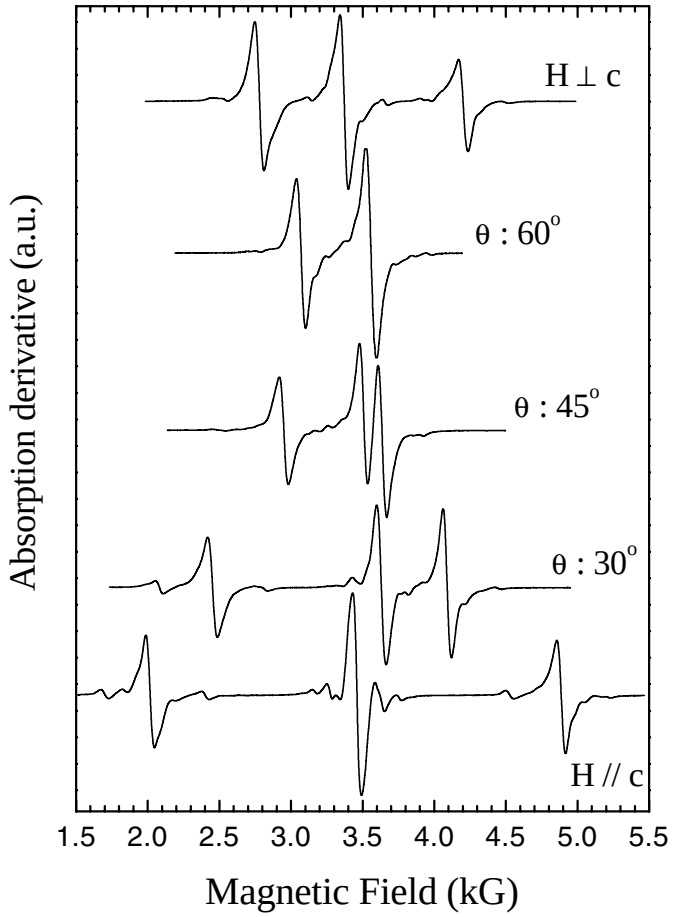

Figure 1. ESR spectra of LiSGaF:Cr at room temperature for magnetic field at different angles relative to the *c*-axis.

For LiSGaF:Cr (2.5%) (not shown) several additional lines have been observed. Their intensities are much smaller than those of the main spectrum, and their angular dependence in the *ac*-plane does not present the expected axial symmetry. These lines have been previously reported for LiSAF:Cr (2%) and LiCAF:Cr (2%) [16, 17], and can be attributed to the presence of weakly coupled pairs of Cr^{3+}.

For LiSAF:Cr, a similar spectrum was obtained, but with a smaller separation between the absorption lines than that observed in LiSGaF:Cr. The dependence of the ESR line position on the external magnetic field orientation is shown in figure 2(b).

The ESR spectrum of Cr^{3+} in axial symmetry is usually explained using the following spin Hamiltonian [19, 20]:

$$\hat{H} = \beta \boldsymbol{S} \cdot \boldsymbol{g} \cdot \boldsymbol{H} + D\left[\hat{S}_z^2 - \frac{1}{3}S(S+1)\right] + \boldsymbol{S} \cdot \boldsymbol{A} \cdot \boldsymbol{I} \tag{1}$$

where β is the Bohr magneton, S is the effective spin of the ground state, $\boldsymbol{g}$ is the gyromagnetic ratio tensor, $\boldsymbol{H}$ is the magnetic field, D is the zero-field splitting axial parameter, $\boldsymbol{A}$ is the hyperfine coupling tensor and $\boldsymbol{I}$ is the nuclear spin.

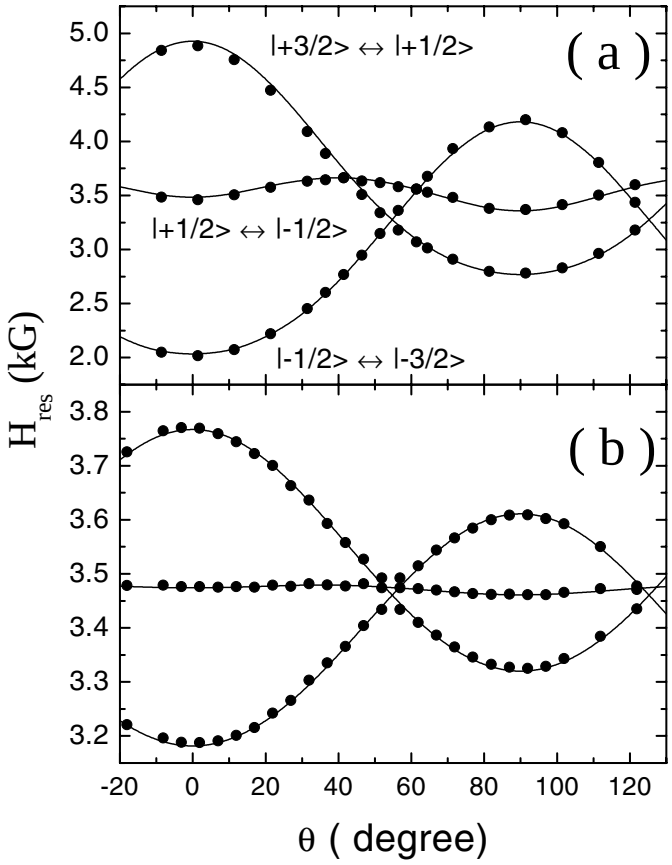

Figure 2. The angular dependence of the resonance magnetic field at room temperature for (a) LiSGaF:Cr and (b) LiSAF:Cr. The solid curves represent the simulation using equation (1) with parameters listed in table 1.

The angular dependence of the principal lines ($I = 0$) at room temperature was simulated by solving equation (1) with an effective spin $S = 3/2$. The results are shown in figure 2 (solid curves) for both compounds and are in good agreement with the experimental data. The hyperfine parameters were estimated either parallel or perpendicular to the *c*-axis and are listed in table 1.

Table 1. ESR parameters from LiSGaF:Cr and LiSAF:Cr at room temperature.

Sample	$g_{\|\|}$	$g_\perp$	$A_{\|\|}$(G)	$A_\perp$(G)	$\|D\|$ (10^{-3} cm^{-1})
LiSGaF:Cr (1.5%)	1.956 (2)	1.960 (3)	160 (5)	150 (20)	64.9 (8)
LiSAF:Cr (1.5%)	1.959 (2)	1.961 (3)	30 (5)	<20	13.4 (3)

The simulation of the resonance field can determine the magnitude of the zero-field splitting (D), but not its sign. Nevertheless, using $2b_2^0 = \lambda(g_{||} - g_\perp)$ [19, 20], where λ is the spin–orbit coupling constant and b_2^0 is the crystal field parameter (Newman's notation [21]), we find that b_2^0 is negative because $g_{||} < g_\perp$ for both compounds. Eremin and Antonova [22] have

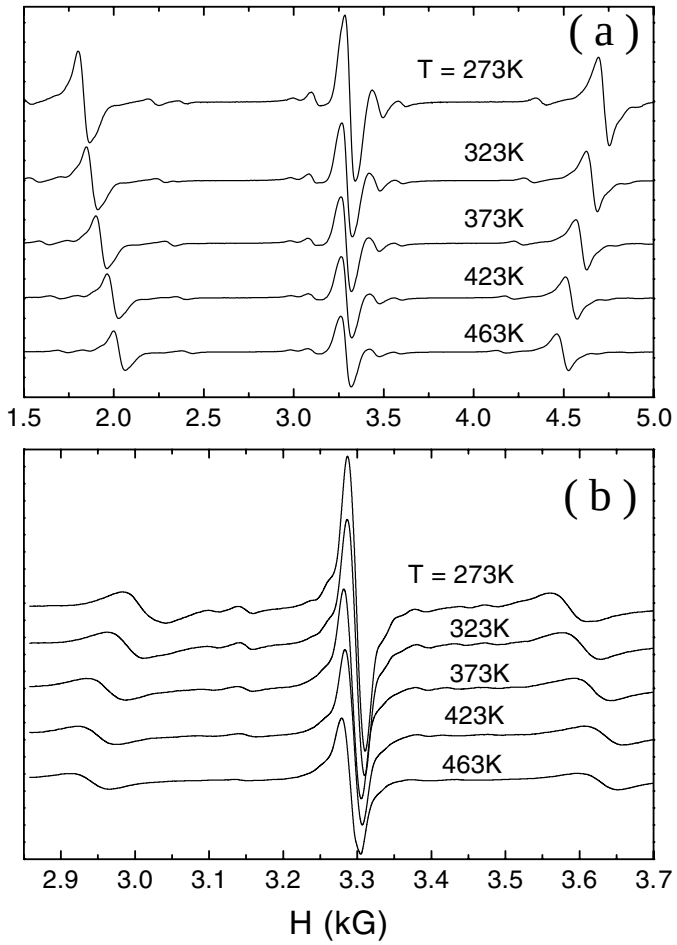

Figure 3. ESR spectrum temperature dependence for (a) LiSGaF:Cr and (b) LiSAF:Cr, with magnetic field along the crystalline *c*-axis.

shown that the signs of b_2^0 and parameter D are opposite, and, therefore, we conclude that D is positive. Yamaga *et al* [16] also obtained $D > 0$ for LiSAF:Cr from the line intensity analysis at low temperatures, in agreement with our results. However, the considerable uncertainty of the g-values makes the determination of the sign of D by this method difficult, and we will restrict our analysis to the magnitude of D.

When the magnetic field is oriented along the crystalline *c*-axis the spin Hamiltonian is diagonal and we can determine $g_{||}$ from the position of the central line ($|+1/2\rangle \leftrightarrow |-1/2\rangle$) and $|D|$ from the separation of the $|\pm 3/2\rangle \leftrightarrow |\pm 1/2\rangle$ transitions. Keeping the magnetic field in that direction we obtained the temperature dependence of the spectrum, which is shown in figures 3(a) and (b) for LiSGaF:Cr and LiSAF:Cr, respectively. The linewidth and shape of the resonance lines do not change with temperature and a small positive g-shift of the central transition was observed with increasing temperature for both compounds. For LiSGaF:Cr the separation of the $|\pm 3/2\rangle \leftrightarrow |\pm 1/2\rangle$ transitions decreases with increasing temperature, showing a reduction in $|D|$-values. In contrast, for LiSAF:Cr, $|D|$ increases with the temperature, as shown in figure 4.

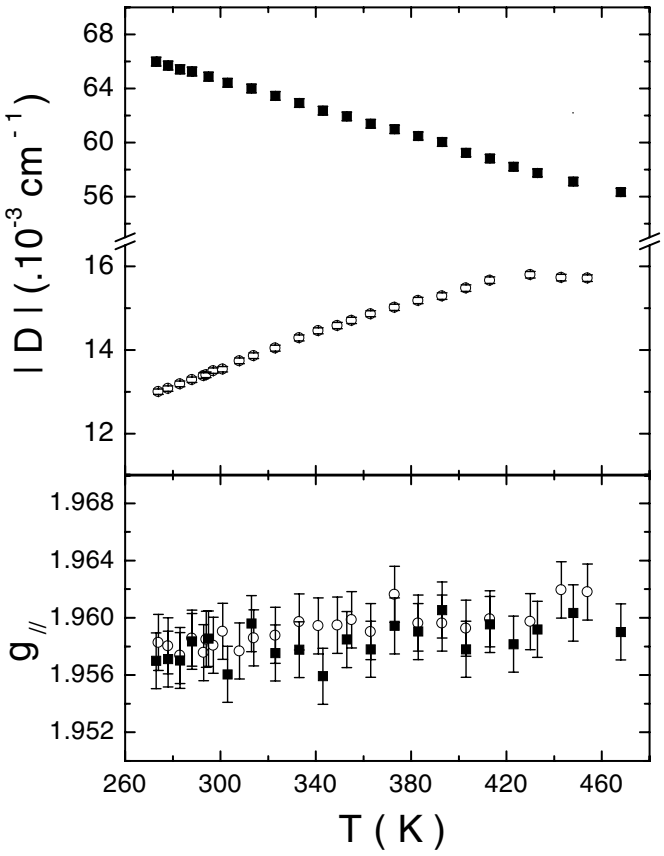

Figure 4. The zero-field splitting axial parameter (top) and $g_{||}$-value (bottom) as functions of temperature for LiSGaF:Cr (■) and LiSAF:Cr (◯) .

3. Discussion

The angular dependence of the resonance field for both compounds shows that the Cr ion occupies a site with axial symmetry along the *c*-axis, and the same result was found for several compounds of this family [16, 17]. The value of the zero-field splitting for LiSAF:Cr at room temperature is in complete agreement with the result reported by Yamaga *et al* [16] ($|D| = 13.5 \times 10^{-3}$ cm^{-1}). For the Ca compound (LiCAF:Cr) the values of $|D|$, listed in table 2, are much greater than those of the Sr compound. This fact was attributed by Yamaga *et al* [16] to a large deviation of the $c/2a$-ratio of the ideal trigonal structure ($c/2a = 1$) [16]. However, x-ray diffraction data show that the F–Al distances in the AlF_6 octahedron are the same, and very similar for different compounds (1.799 Å for LiSAF and 1.800 Å for LiCAF). Moreover, considering that $|D|$ is proportional to this deviation, LiSGaF:Cr should have the smaller value. Nevertheless, this compound presents an intermediary value for $|D|$, and this implies that other contributions should be considered to explain the results.

X-ray diffraction results [11–14] show that the distortion of the Cr^{3+} site in doped materials is associated with the relative rotation of the two trigonal F faces. In table 2 we show the twist angles $\Delta\theta(\theta - 60^\circ)$ obtained for different compounds [13, 14]. One can observe that $\Delta\theta$ is larger in LiSGaF than in LiSAF, indicating a larger distortion on the first compound, in

agreement with the ESR results. However, LiCAF presents smaller twist angles and a small $|D|$-value is expected, in contrast with the ESR experiments.

Results obtained for LiCAF and LiSAF doped with S ions (Fe^{3+} and Gd^{3+}) [22, 24] show a larger $|D|$-value for Sr compounds, in agreement with the $\Delta\theta$ tendency, but in contrast with the Cr^{3+}-doped compounds. These results show that dynamic distortion, such as the dynamic Jahn–Teller effect, can be important for this family of compounds.

In table 2 we can observe a correlation between $|D|$ and the fluorescence lifetime, or emission cross section. This correlation can be explained considering that the dynamic effect which distorted the ground state will also affect the excited state, changing the $^4T_2$–$^4A_2$ transition probability. Payne *et al* [2] showed that the static distortion of the Al site of Cr^{3+}-doped compounds gives rise to the polarization characteristic of the absorption and emission spectra, while the dynamic distortion also provides a contribution to the absorption strength and the emission lifetime. Also, analysis of the spin–orbit components of the $^4T_2$ state revealed the importance of the dynamic Jahn–Teller distortion.

Table 2. Physics parameters of colqueriite compounds.

	$\|D\|$ (10^{-3} cm^{-1})	$c/2a$ [23]	$\Delta\theta$ [13, 14] ($^\circ$)	τ [7] (μs)	Ω_{emission} [7] (10^{-22} cm^2)	α_a [26, 27] ($10^{-6}\,^\circ$C^{-1})	α_c [26, 27] ($10^{-6}\,^\circ$C^{-1})
LiSAF:Cr	13.4	1.004	7.2	67	4.8	25	−10
LiSGaF:Cr	64.9	1.001	8.2	88	3.3	12	0
LiCAF:Cr	101 [16]	0.963	3.4	205	1.2	22	3.6

$|D|$, zero-field splitting; $c/2a$, lattice parameter ratio; $\Delta\theta = \theta - 60^\circ$, twist angles of D_3; τ, fluorescence lifetime; Ω_{emission}, emission cross section; α_a and α_c, thermal expansion coefficients.

Figure 4 shows that $|D|$ increases with the increase of the temperature for LiSAF:Cr and the same behaviour was reported by Yamaga *et al* [16] for a different temperature range. In contrast, for LiSGaF:Cr, $|D|$ decreases with increasing temperatures. A decrease of $|D|$ for LiCAF:Cr is reported for temperatures between 1.3 and 300 K [16].

The thermal behaviour of $|D|$ for these compounds can be understood considering the distortion associated with the relative rotations of the two trigonal F faces and the thermal expansion coefficients. For an octahedron with O_h symmetry, the angle between these faces is 60°. Because the A atoms (Sr or Ca) are placed at the vertices of a distorted trigonal prism surrounding the M atom (Al or Ga), bigger A–F distances produce greater deviation of the twist angle θ from 60° [14].

The thermal expansion coefficients for LiCAF and LiSGaF are positive, and when the temperature increases the distance A–F (Ca–F or Sr–F) also increases. Therefore, the interaction A–F decreases, resulting in small rotations of the trigonal F faces, leading consequently to a small $|D|$-value.

For LiSAF, in contrast, the c-axis thermal expansion coefficient (α_c) is negative and the increase of the temperature reduces the Sr–F distance, leading to bigger rotations and consequent increase of $|D|$. The saturation tendency of $|D|$ observed above 400 K in figure 4 indicates that the α_c signal is changed. However, the temperature behaviour of thermal expansion coefficients in this temperature range is not known and further investigation is necessary.

The ESR spectra as functions of the temperature show a constant linewidth, implying that the spin–lattice relaxation for the ground state is independent of the temperature. A similar behaviour is expected for the relaxation of the excited states. Therefore, the temperature dependence of the fluorescence lifetime observed in these compounds [4, 10, 25] cannot be

explained by spin–lattice relaxation changes, and more detailed studies of the thermal quenching of fluorescence in these materials are necessary to clarify which mechanism is responsible for the temperature dependence.

4. Conclusions

ESR measurements in LiSAF:Cr and LiSGaF:Cr show that the Cr site has axial symmetry for both compounds. The magnitude of the zero-field splitting $|D|$ is bigger in LiSGaF:Cr, in agreement with rotations of the trigonal F faces obtained by x-ray diffraction. The comparison of $|D|$ between compounds with Sr and Ca shows that dynamic effects can be important in this family of crystals.

Our results show that for LiSGaF:Cr, the parameter $|D|$ decreases with increasing temperature. In contrast, for LiSAF:Cr, D increases with the temperature. This different thermal behaviour can be explained considering the opposite sign of thermal expansion coefficient of the c-axis.

Acknowledgments

The authors are grateful to Brazilian Agencies CNPq and FAPESP for partial financial support of this work.

References

[1] Payne S A, Chase L L, Newkirk H W, Smith L K and Krupke W F 1988 *IEEE J. Quantum Electron.* **24** 2243
[2] Payne S A, Chase L L and Wilke G D 1989 *J. Lumin.* **44** 167
[3] Beaud P, Richardson M C, Chen Y F and Chai B H T 1994 *IEEE J. Quantum Electron.* **30** 1259
[4] Balembois F, Falcoz F, Kerboull F, Druon F, Georges P and Brun A 1997 *IEEE J. Quantum Electron.* **33** 269
[5] Payne S A, Smith L K, Beach R J, Chai B H T, Tassano J H, DeLoach L D, Kway W L, Solarz R W and Krupke W F 1994 *Appl. Opt.* **33** 5526
[6] Uemura S and Miyazaki K 1997 *Japan J. Appl. Phys.* **36** 4312
[7] Smith L K, Payne S A, Kway W L, Chase L L and Chai B H T 1992 *IEEE J. Quantum Electron.* **28** 2612
[8] Sorokina I T, Sorokin E, Witner E, Cassanho A and Jenssen H P 1996 *Opt. Lett.* **21** 204
[9] Yanousky V P, Wise F W, Cassanho A and Jenssen H P 1995 *Opt. Lett.* **20** 1304
[10] Balembois F, Druon F, Falcoz F, Georges P and Brun A 1997 *Opt. Lett.* A **22** 387
[11] Viebahn V W 1971 *Z. Anorg. (Allg.) Chem.* **386** 335
[12] Knox K 1960 *Acta Crystallogr.* **13** 507
[13] Schaffers K I and Keszler D A 1991 *Acta Crystallogr.* C **47** 18
[14] Yin Y and Keszler D A 1993 *Mater. Res. Bull.* **28** 1337
[15] Lee H W H, Payne S A and Chase L L 1989 *Phys. Rev.* B **39** 8907
[16] Yamaga M, Henderson B, Holliday K, Yosida T, Fukui M and Kindo K 1999 *J. Phys.: Condens. Matter* **11** 10499
[17] Holliday K, Russell D L, Nicholls J F H, Henderson B, Yamaga M and Yosida T 1998 *Appl. Phys. Lett.* **72** 2232
[18] Sorokinina I T, Sorokin E, Wintner E, Noginov M A, Szipöcs R, Cassanho A and Jenssen H P 1997 *Laser Phys.* **7** 187
[19] Abragam A and Bleaney B 1970 *Electronic Paramagnetic Resonance of Transition Ions* (Clarendon: Oxford)
[20] Laguta V V, Antimirova T V, Glinchuk M D, Bykov I P, Rosa J, Zaritskii V and Jastrabík L 1997 *J. Phys.: Condens. Matter* **9** 10 041
[21] Newman D 1971 *J. Adv. Phys.* **20** 197
[22] Eremin M V and Antonova I I 1998 *J. Phys.: Condens. Matter* **10** 5567
[23] Yin Y B and Keszler D A 1992 *Chem. Mater.* **4** 645

[24] Abdulsabirov R Yu, Antonova I I, Korableva S L, Nizamutdinov N M, Stepanov V G and Khasanova N M 1997 *Phys. Solid State* **39** 423
[25] Stalder M, Bass M and Chai B H T 1992 *J. Opt. Soc. Am.* B **9** 2271
[26] Perry M D, Payne S A, Ditmire T, Beach R, Quarles G J, Ignatuk W, Olson R and Weston J 1993 *Laser Focus World* **85**
[27] Cassanho A and Jenssen H 1997 *Laser Focus World* **169**